PAPER

Check for updates

Catalytic activity and stability of NiPt/C catalysts for the synthesis of iso-butanol from methanol/ethanol mixtures†

Joachim Pasel, [iD] *[a] Johannes Häusler,[ab] Ralf Peters [iD] [acd] and Detlef Stolten[b]

Mixtures of sustainably produced ethanol and methanol can serve as educts for the synthesis of higher alcohols, which are considered carbon-neutral components and feedstocks for the transportation and chemical sectors. In this respect, this study focused on bi-metallic NiPt catalysts supported on activated carbon for the synthesis of iso-butanol. Reaction temperature, time on stream, and the inlet concentration of ethanol were varied to investigate the influence of these parameters on ethanol conversion, the selectivities towards iso-butanol, and other reaction products, as well as the space–time yield of the NiPt/C catalyst. In addition, kinetic parameters were determined. It was found that a reaction temperature of 165 °C was most suitable for the selectivity towards iso-butanol. Activation energies were calculated to the range between 110 kJ mol^{-1} and 120 kJ mol^{-1}. TEM experiments revealed that there was no ageing of the catalytically active species of the $Ni_{99}Pt_1$/C catalyst during iso-butanol synthesis.

Introduction

The catalytic upgrading of mixtures of methanol and ethanol (synthesized from green H_2 and CO_2 being separated from various industrial exhaust streams) to carbon-neutral higher alcohols ($>C_4$) is increasingly important, as these alcohols are valuable as components in future fuels and for the chemical industry. For instance, iso-butanol possesses similar physico–chemical characteristics to conventional gasoline.[1] Long-chain unbranched fatty alcohols ($>C_{10}$) are used in the chemical industry as raw materials for lubricant additives.[1] In this area, Häusler *et al.*[2,3] and Pasel *et al.*[4,5] investigated the synthesis, characterization, and catalytic activity of monometallic (Pt, Cu, Pd, Rh, Ru, Ir) and bimetallic (NiPt, FePd, FePt, CuNi, and CuFe) catalysts for the reaction of ethanol/methanol blends into iso-butanol *via* the Guerbet reaction. The mechanistic course of this reaction is depicted in Fig. 1. The catalysts were each applied to an activated

carbon support. If compared to each other, the versatile class of bimetallic catalysts proved predominant among the corresponding monometallic host materials, as it offers the option to tailor its geometric and electronic properties and establish beneficial and synergistic metal–metal interactions, which lead to improved catalytic activities and stabilities.[6–10] Therefore, in this study, the focus is on the deeper understanding of the catalytic behavior of an $Ni_{99}Pt_1$/C catalyst with a total weight metal loading (Ni plus Pt) of 5%, as it proved to be the most active and stable in the work mentioned above. Since deactivation with restructuring was found in the monometallic Pt/C catalyst over the experimental period,[3] the $Ni_{99}Pt_1$/C catalyst was examined in detail after the reaction using TEM. Additionally, the influence of catalyst synthesis is discussed and evaluated in terms of catalytic activity. A detailed comparison of the catalytic activity of the $Ni_{99}Pt_1$/C catalyst with that of the main representatives of the Guerbet catalysts[11–19] at the end of the discussion section highlights that a low reaction temperature of 165 °C for the Guerbet reaction to iso-butanol in methanolic solution and a low precious metal mass fraction constitute the uniqueness and innovation of the $Ni_{99}Pt_1$/C catalyst.

With respect to catalysts for the formation of iso-butanol from ethanol/methanol mixtures other than NiPt/C, the patent literature discloses several contributions. For the patent by Fuchs and Querfurth,[20] a mixture of methanol and ethanol vapor was passed over a MgO catalyst at normal and over pressure and temperatures between 200 °C and 400 °C. The activity of the MgO could be increased by adding Th, Pb, Ag, U, Cd, Sn, Cr, Mn, Zn, Fe, Ni, Co, Cu and their oxides or mixtures

[a] Institute of Energy Technologies, IET-4: Electrochemical Process Engineering, Forschungszentrum Jülich GmbH, 52425 Jülich, Germany.
E-mail: j.pasel@fz-juelich.de, ra.peters@fz-juelich.de; Tel: +49 2461 61 5140
[b] Chair for Fuel Cells, Faculty of Mechanical Engineering, RWTH Aachen, 52062 Aachen, Germany
[c] Synthetic Fuels, Faculty of Mechanical Engineering, Ruhr-Universität Bochum, Universitätsstr. 150, 44801 Bochum, Germany
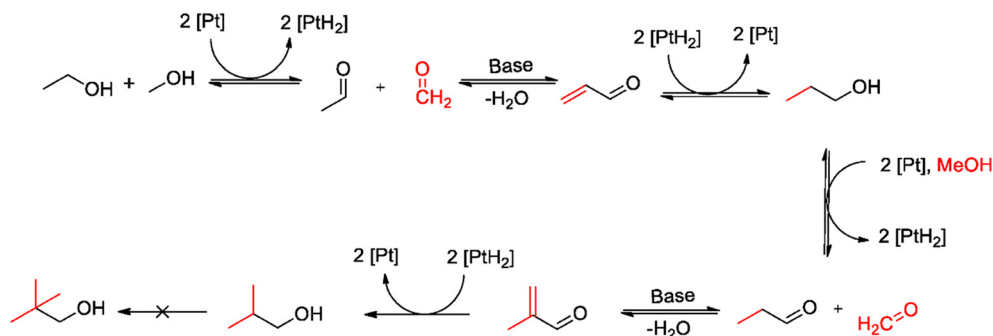*[d] Jülich-Aachen-Research-Alliance, Wilhelm-Johnen-Straße, 52425 Jülich, Germany*

Fig. 1 Mechanistic course of the formation of iso-butanol *via* the Guerbet reaction.[37]

of these components. Different mixing ratios of methanol, ethanol and hydrogen are described. A different patent[21] describes the synthesis and the process to produce iso-butanol on bimetallic catalysts on basic support materials such as MgO, ZrO$_2$, TiO$_2$, MgAl hydrotalcite, fluorapatite, ZnO, SrO, BaO and CeO$_2$. The metal alloys consisted of one or more of the metals Pd, Ni, Rh, Pd, Co, Cu, Pt, Mo, and W. For example, the PtNi/MgO catalyst with a metal loading of 5% to 10% showed ethanol conversions of 65% at temperatures of 350 °C to 450 °C. The selectivity towards iso-butanol was up to 75% at a liquid hourly space velocity of 1 h^{-1}. Vanderspurt and Kao[22] report about the combined conversion of ethanol and methanol in the presence of synthesis gas. Large-pored mordenites loaded with precious metals and alkali metals were used for the synthesis of iso-butanol from ethanol and methanol in the presence of syngas. With a catalyst exchanged with Li ions, conversions of ethanol up to 96% with a selectivity towards iso-butanol of 61% were found. By-products were n-propanol, gaseous hydrocarbons, and other higher alcohols (C$_{4+}$). The reaction temperature in this case was 351 °C, the H$_2$/CO ratio amounted to 0.9, and the gas hourly space velocity was 8450 h^{-1}. In a different patent,[23] the authors describe the synthesis of a MnZrZn oxide catalyst doped with Pt and Pd. In a gas-phase reaction in the presence of synthesis gas, methanol and ethanol were converted to iso-butanol at 330 °C to 355 °C. In the experimental examples, ethanol conversions of up to 99.5% at 380 °C are described with the PdMn$_{0.38}$Zn$_{0.26}$Zr$_{0.30}$-Li$_{0.06}$ catalyst. The composition of the product was 62.1 vol% methanol, 30.8 vol% iso-butanol, 2.1 vol% methyl-butanol, 0.4 vol% ethanol and 1.9 vol% *n*-propanol. Carlini *et al.*[24] describe the synthesis of iso-butanol from methanol and propanol using Cu-chromite catalysts and a hydrotalcite-based MgAl support with different compositions. This support was water-tolerant and showed a good yield with almost quantitative selectivity to iso-butanol at 300 °C. In subsequent work, the reaction temperature was lowered by 100 K with the same selectivity and yield by using Cu–MgAl catalysts.[25] In an earlier work of this group,[26] they used the Cu-chromite catalyst with MeONa as basic component and found a selectivity towards iso-butanol of 98% with 61% ethanol conversion.

Tsuchida *et al.*[27] present a detailed investigation about the application of Ca$_3$(PO4)$_2$ based catalysts with different Ca/P

ratios, which can be either hydrotalcites or hydroxyapatites. As an example, a mixture of methanol and ethanol in a ratio of 1 : 1 reacted at a contact time of 1 second on a hydroxyapatite catalyst at temperatures from 100 °C to 500 °C and normal pressure. At 155 °C, this resulted in an ethanol conversion of 0.1%, while the selectivity to 1-propanol was 43.3%. Unsaturated C$_4$ alcohols were produced with a selectivity of 44.8%. At temperatures from 357 °C to 509 °C, the selectivities towards the alcohols decreased, while the formation of olefins and aromatics increased. Hydrotalcite-based catalysts containing the metals Co, Ni, Cr and Pt in different compositions were produced by Kourtakis *et al.*[28] Gaseous methanol/ethanol mixtures reacted at temperatures between 300 °C and 400 °C and pressures between 0.1 MPa and 20.7 MPa in the catalyst bed. The highest conversions of ethanol were achieved with the Pt-hydrotalcite catalyst, with values of 76.6% at 300 °C (selectivity towards iso-butanol of 13.4%) up to 91.7% at 400 °C (selectivity towards iso-butanol of 8.3%). The reaction temperature is inversely proportional to the selectivity to iso-butanol, while the conversion of ethanol increased with increasing temperature. To date, only a few studies have been carried out on the synthesis of iso-butanol from ethanol/methanol mixtures in the liquid phase using heterogeneous catalysts. Liu *et al.*[29] present an Ir-containing catalyst that has a "yolk–shell" structure. This structure comprises an inner core of mesoporous carbon and a thinner, equally mesoporous shell. The catalyst achieved a TON (turnover number) of 9259 h^{-1} and a TOF (turnover frequency) of 257 h^{-1} after 36 h at 170 °C. KOH was used as the base. Siddiki *et al.*[30] used NaOH as a dissolved base for the methylation of alcohols, ketones and indoles with methanol in a liquid-phase reaction with Pt/C as a heterogeneous catalyst. The catalyst with 5% Pt/C showed the highest formation rate for all compound classes compared to other carbon-supported transition metal catalysts. The methylation rate as a function of H$_2$ adsorption energies showed an increase from Re < Ru = Ni < Pd < Rh < Pt in the range of −3.2 eV to −2.8 eV. The graphical representation results in a volcano curve for the activity of the metals, which is typical for the Brønsted–Evans–Polanyi (BEP) relationship.[31] Gupta *et al.*[32] investigated P,N-type phosphaalkene-based Ir complexes for the reaction between ethanol and methanol forming iso-butanol. In a reaction over 20 hours, they achieved 60% iso-

This journal is © The Royal Society of Chemistry 2024

Catal. Sci. Technol., 2024, **14**, 7048–7060 | **7049**

butanol yield with 93% selectivity towards iso-butanol. Liu et al.[17] also used Ir as active component being deposited on nitrogen functionalized carbon materials for the iso-butanol synthesis from ethanol and methanol in the presence of water. They found a selectivity towards iso-butanol higher than 90% at ethanol conversion >50%. The authors stress the importance of a uniform dispersion of very small Ir particles on the surface of the support. Ueda and his co-workers[33] investigated various metal oxide catalysts in the temperature range between 340 °C and 390 °C. The most promising MgO sample achieved 60% ethanol conversion and 46% selectivity towards iso-butanol. Wingad et al.[34] worked with various Ru diphosphine complexes. The best results of 99.8% selectivity towards iso-butanol and more than 75% ethanol conversion were obtained at 180 °C and after 20 hours of time on stream. Olson et al.[35] synthesized a MgO loaded commercial activated carbon and deposited small amounts of Ni onto the surface. This catalyst achieved an ethanol conversion of 100% and a yield of iso-butanol of 90% at 360 °C. Homogeneous catalyst systems for iso-butanol synthesis from ethanol and methanol are presented by Messori et al.[36] They present bi-functional catalysts based on Ru, Ir and Mn complexes with different ligands, such as phosphine, bidentate bisphosphine, and cyclopentadienone.

Experimental

The 5 wt% $Ni_{99}Pt_1$/C catalyst was characterized in detail in ref. 2. In this paper, also turn-over frequencies for this catalyst are given and compared to those of other bimetallic activated carbon supported samples.

Catalyst synthesis

For the synthesis of the 5 wt% $Ni_{99}Pt_1$/C catalyst, the activated carbon support was weighed and impregnated with a precursor solution containing the calculated quantities of $[Pt(NH_3)_4](NO_3)_2$ (Thermo Scientific) and $Ni(NO_3)_2 \cdot 6H_2O$ (Acros Organics). The wetted activated carbon (Sigma-Aldrich) was homogenized by shaking. Following impregnation, the catalyst precursor was dried on a rotary evaporator at 40 mbar and a 40 °C water bath temperature. It was then calcined at 500 °C in an N_2 stream for four hours and finally reduced in a volume flow of 2% H_2 in N_2 at 250 °C for one hour.

The $Ni_{99}Pt_1$@C catalyst from Table 1 was synthesized by the precipitation of Ni on the activated carbon support. For this purpose, $Ni(NO_3)_3$ was dissolved as a precursor in deionized water and precipitated as $Ni(OH)_3$. The product was aged for one hour at room temperature under stirring, filtered off, and washed with deionized water. After drying, the material was impregnated with an aqueous solution of $[Pt(NH_3)_4](NO_3)_2$, dried again, calcined at 500 °C for four hours in an N_2 stream, and then reduced in a volume flow of 2% H_2 in N_2 at 250 °C for one hour.

The catalyst Ni/C from Table 1 was prepared in the same way as the 5 wt% $Ni_{99}Pt_1$/C catalyst, but without the addition of $[Pt(NH_3)_4](NO_3)_2$ to the precursor solution.

Transmission electron microscopy TEM

As a first step, the powder samples were applied to a Cu-TEM grid. To record the high-angle annular dark field (HAADF) and energy-dispersive X-ray analysis (EDX) images an aberration-corrected FEI Titan G2 80 to 200 TEM field emission electron microscope was used in conjunction with a Super-X EDX system at 200 eV. For lower resolutions, an FEG TEM Hitachi HF5000 (Hitachi Europe GmbH, Düsseldorf, Germany) with an acceleration voltage of 200 eV was employed.[3]

Carrying out the activity tests

To prepare the reaction solution, 1.8 g of NaOH (45 mmol) and 2.8 g of ethanol (60 mmol) were dissolved in methanol in a 100 ml volumetric flask. In addition, n-decane was added as an internal standard. In the autoclave (Parr Instrument Company, Moline, USA), 70 ml of the reaction solution and 250 mg of the dry catalyst ($\emptyset_{particle}$ < 75 μm) were weighed. The autoclave was sealed and pressurized three times with 6 bar N_2 to exchange the atmosphere. The impeller stirrer was then switched on at 1000 RPM. The time on stream was four hours and started when the desired reaction temperature was reached. At regular intervals of 30 minutes, samples were taken from the reactor vessel to determine the reaction's progress.

Analysis via gas-chromatography GC

Details of the way in which the GC analyses for this work were carried out can be found in the publication of Häusler et al.[3]

Calculations

The calculation of ethanol conversion was performed using the sum of the concentrations of the different liquid

Table 1 Selectivities towards, and yields of, the main products from the catalytic experiments with differently-synthesized 5 wt% $Ni_{99}Pt_1$/C catalysts and a monometallic 5 wt% Ni/C sample, m(catalyst) = 250 mg, d(powder) < 75 μm, V(reactor) = 70 ml, T = 150 °C, c(NaOH) = 450 mmol l^{-1}, c(n-decane) = 15 mmol l^{-1}, c(ethanol) = 1600 mmol l^{-1}, time on stream: 4 h, methanolic solution

Catalyst [—]	X_{EtOH} [%]	$S_{1\text{-propanol}}/Y_{1\text{-propanol}}$ [%]	$S_{iso\text{-BuOH}}/Y_{iso\text{-BuOH}}$ [%]	$S_{1\text{-BuOH}}/Y_{1\text{-BuOH}}$ [%]	$S_{2\text{-methyl-butan-1-ol}}/Y_{2\text{-methyl-butan-1-ol}}$ [%]
Ni/C	0.07	23.57/0.02	—	18.90/0.01	—
$Ni_{99}Pt_{1\ calc}$/C^a	0.60	4.37/0.03	52.95/0.32	5.90/0.04	21.74/0.13
$Ni_{99}Pt_{1\ red}$/C^b	0.82	13.82/0.03	75.23/0.62	—	16.36/0.16
$Ni_{99}Pt_1$@C^c	1.29	1.89/0.02	85.88/1.10	—	11.12/0.14

^{a} 2-Ethylbutan-1-ol: S = 15.03%, Y = 0.09%. ^{b} Acetone: S = 13.19%, Y = 0.03%. ^{c} Acetone: S = 1.11%, Y = 0.01%.

products. In eqn (1), c_k stands for their respective concentrations and Z represents their stoichiometric coefficients for the formation from ethanol and methanol, respectively.

$$X(\text{ethanol}) = 1 - \frac{\sum\limits_{k=i}^{n} c_k \cdot Z}{c(\text{ethanol}),\ t = 0} \quad (1)$$

The yield Y_i of a specific component "i" was calculated using the quotient of the measured concentration of product i and the calculated ethanol concentration of the feed solution.

$$Y_i = \frac{c_i \cdot Z}{c(\text{ethanol}),\ t = 0} \quad (2)$$

The selectivity S_i towards product "i" was calculated according to the following equation:

$$S_i = \frac{c_i \cdot Z}{\sum\limits_{k=i}^{n} c_k \cdot Z} \quad (3)$$

The space–time yield of iso-butanol is defined as the quotient of the number of moles of iso-butanol formed and the product of the catalyst mass and time on stream.

$$\text{STY} = \frac{n(\text{iso-ButOH})}{m(\text{cat}) \cdot t_R} \quad (4)$$

The activation energy of the reaction can be determined for constant inlet concentrations of ethanol without determining the pseudo reaction order "a," the pseudo rate constant "k," and the pre-exponential factor "A" by extending and then simplifying the equation for the logarithmic rate law as follows:

$$\ln(v_0) = \ln(k) + a \cdot \ln(c_0(\text{ethanol})) \quad (5)$$

$$k = A \cdot e^{-E_A/(R \cdot T)} \quad (6)$$

$$\ln(v_0) = \ln(A) - \frac{E_A}{R \cdot T} + a \cdot \ln(c_0(\text{ethanol})) \quad (7)$$

$$\ln(v_0) = C - \frac{E_A}{R} \cdot \frac{1}{T} \quad (8)$$

The formation rates "r" in Table 3 for the catalysts in entries 13 to 18 were calculated using eqn (9). In this equation, $A(\text{BET})$ is the specific surface area being calculated *via* the method of Brunnauer–Emmett–Teller.[38]

$$r = \frac{c(\text{ethanol})}{A(\text{BET}) \cdot t_R} \quad (9)$$

Results and discussion

Influence of the synthesis method on the catalytic activity

To determine the influence of the synthesis methods of impregnation and precipitation, whose details are explained in the Experimental section, the catalytic behavior of the Ni$_{99}$Pt$_1$/C catalyst was investigated when it was prepared using these two different routes (see Table 1). As the reference case, the results from the Pt-free Ni/C sample were also collected and are displayed in the first line of Table 1.[2] It becomes obvious that ethanol conversion was very low, and no iso-butanol was formed with the Ni/C catalyst. The main product was acetaldehyde (not shown in Table 1).[2] The second line displays the results with the impregnated Ni$_{99}$-Pt$_1$/C sample, which was calcined but not reduced. In this case, ethanol conversion was slightly increased to 0.60% at a selectivity towards iso-butanol of approximately 53%. By-products that formed in significant quantities included 1-propanol, 1-butanol, 2-methylbutan-1-ol, and 2-ethylbutan-1-ol.[2] The impregnated, calcined, and reduced Ni$_{99}$Pt$_1$/C catalyst in the third line showed a further increase in ethanol conversion and selectivity towards iso-butanol, as well as additionally the formation of acetone with a selectivity of 13.19%. For the formation of acetone, 2 moles of acetaldehyde reacted to form 3-hydroxybutanal which in turn decomposed into acetone and CO.[39] 1-Propanol as an important starting material for iso-butanol was generated with a selectivity of 13.82%.

The Ni$_{99}$Pt$_1$/C sample from the fourth line in this table, whose Ni component was not impregnated but precipitated, showed increased ethanol conversion of 1.29% and selectivities of 1.11% towards acetone, 1.89% towards 1-propanol, and 11.12% towards 2-methylbutan-1-ol. Iso-butanol was the main product, with a selectivity of 85.88%. From the finding that the selectivity towards acetone with the precipitated catalyst was much lower than that of the impregnated, calcined, and reduced Ni$_{99}$Pt$_1$/C catalyst (1.11% *vs.* 13.19%), a reduced fragmentation of previously formed higher alcohols in the case of the precipitated sample can be concluded. The significantly lower selectivity towards 1-propanol of the precipitated Ni$_{99}$Pt$_1$/C is a positive finding, as it can be derived that the formation and methylation of 1-propanol took place at higher reaction rates, thus leading to a higher selectivity towards iso-butanol. An increased rate for the dehydrogenation of ethanol on the Ni$_{99}$Pt$_1$@C catalyst with the same methylation rate as on the Ni$_{99}$Pt$_{1\text{red}}$/C catalyst would lead to higher acetaldehyde concentrations with the Ni$_{99}$Pt$_1$@C sample. As a result, the condensation reaction of two moles of acetaldehyde and the subsequent hydrogenation would also increase the concentrations of 1-butanol and the resulting methylation product 2-methylbutan-1-ol. As 2-methylbutan-1-ol can also be formed through the condensation and re-hydrogenation of acetaldehyde and propanal, the lower concentration of 2-methylbutan-1-ol in the case of the Ni$_{99}$Pt$_1$@C catalyst proves the assumption that the methylation reaction proceeds more rapidly on the precipitated catalyst.

This journal is © The Royal Society of Chemistry 2024

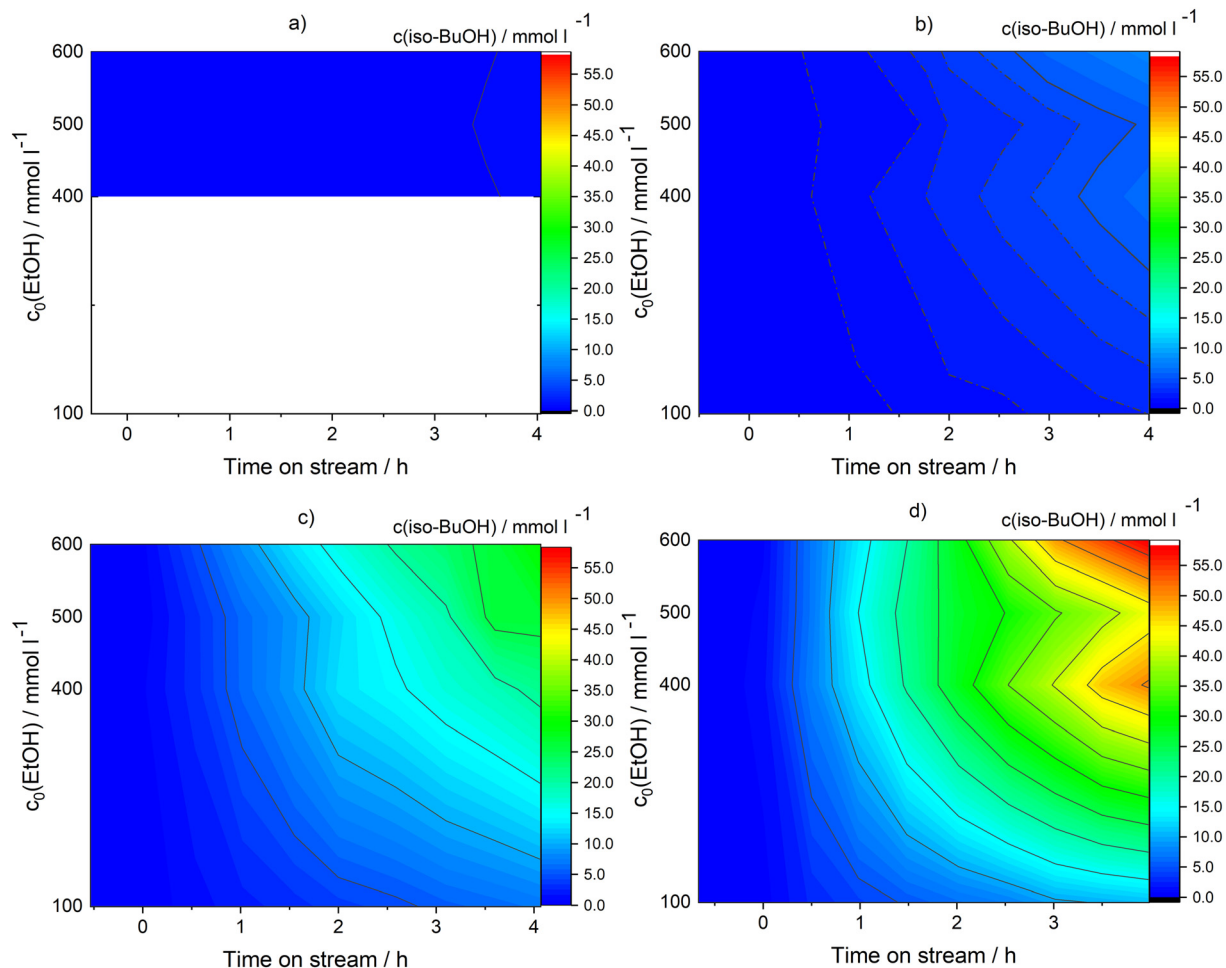*Catal. Sci. Technol.*, 2024, **14**, 7048–7060 | **7051**

Fig. 2 Concentrations of iso-butanol as a function of time on stream and the inlet concentrations of ethanol at different temperatures: a) T = 120 °C; b) T = 150 °C; c) T = 165 °C; d) T = 180 °C, catalyst: 5 wt% $Ni_{99}Pt_1$/C, m(catalyst) = 250 mg, d(powder) < 75 μm, V(reactor) = 70 ml, c(NaOH) = 450 mmol l^{-1}, c(n-decane) = 15 mmol l^{-1}, methanolic solution.

Influence of reaction parameters on iso-butanol concentrations

To investigate the influence of the reaction temperature, the inlet concentration of ethanol in the reaction mixture and the time on stream, respectively, on the formation of iso-butanol on the 5 wt% $Ni_{99}Pt_1$/C catalyst, reaction temperatures of 120 °C, 150 °C, 165 °C, and 180 °C were applied, while the initial ethanol concentrations were set to 100 mmol l^{-1}, 400 mmol l^{-1}, 500 mmol l^{-1}, and 600 mmol l^{-1}. The time on stream was a maximum of four hours, with a sample being taken for analysis every 30 minutes. In this respect, it becomes obvious from part (a) of Fig. 2 that during the four hours of time on stream at 120 °C, the concentration of iso-butanol was almost independent of the inlet concentration of ethanol. At this temperature, the maximum final concentration of iso-butanol was only 0.55 mmol l^{-1} at an inlet concentration of ethanol of 500 mmol l^{-1}. Given that, at 120 °C only very low iso-butanol concentrations close to the quantification limit of the gas-chromatograph were measured at an ethanol inlet

concentration of 400 mmol l^{-1}, no experiment was carried out at an inlet ethanol concentration of 100 mmol l^{-1} at this temperature. For better comparability of the diagrams, however, their design was always kept the same. As there was no measurement in the range from 100 mmol l^{-1} to 400 mmol l^{-1} at 120 °C, this area is shown in white. However, at an increased reaction temperature of 150 °C (see part (b) of Fig. 2), higher final concentrations of iso-butanol were observed when the inlet ethanol concentration was 400 mmol l^{-1} or higher. The maximum concentration amounted to approximately 8 mmol l^{-1} after a reaction time of four hours and an inlet concentration of ethanol of 600 mmol l^{-1}. This is more than ten times higher than at a reaction temperature of 120 °C. It is noteworthy that at 150 °C, the concentrations of iso-butanol were consistently higher at an inlet ethanol concentration of 400 mmol l^{-1} than at 500 mmol l^{-1}. This is due to measurement inaccuracies. At 165 °C (see part (c) of Fig. 2), the positive effect of an enhanced reaction temperature becomes more evident. An iso-butanol concentration of 5 mmol l^{-1} was already reached after 2.75 hours of time on stream, even

with an ethanol inlet concentration of 100 mmol l^{-1}. It becomes clear from this diagram that an increased ethanol inlet concentration caused a higher formation of iso-butanol, with a maximum of approximately 30 mmol l^{-1} at the highest ethanol inlet concentration and after 4 hours of time on stream. At a reaction temperature of 180 °C, the highest formation of iso-butanol was achieved (see part (d) of Fig. 2). In this case, the concentration of iso-butanol of 5 mmol l^{-1} was already reached after 1.5 hours of time on stream for the inlet ethanol concentration of 100 mmol l^{-1}, and even after 0.5 hour at ethanol concentrations between 400 mmol l^{-1} to 600 mmol l^{-1}. Iso-butanol concentrations in the range of approximately 50 mmol l^{-1} to 60 mmol l^{-1} were observed after 4 hours of time on stream and with ethanol inlet concentrations of 400 mmol l^{-1} and 600 mol l^{-1}, respectively. Just as with 180 °C, the concentrations of iso-butanol were in most cases higher at an inlet ethanol concentration of 400 mmol l^{-1} than at 500 mmol l^{-1}. The measurement series with 500 mmol l^{-1} inlet concentration of ethanol can be regarded as a slight deviation from the general trend. In summary, Fig. 2 shows that all three factors, namely the inlet concentration of ethanol, the reaction temperature, and the time on stream significantly influenced the final concentration of iso-butanol. Thereby, the increase in temperature had a stronger effect than enhancing the initial concentration of ethanol. All experimental data for Fig. 2 are summarized in Tables S1–S4.† It is noteworthy that catalyst deactivation was not observed during any of the experiments. Therefore, the concentration increases of iso-butanol occurred linearly over the entire reaction period and across all temperatures and initial concentrations of ethanol.

Influence of reaction parameters on ethanol conversion, iso-butanol yield, selectivity towards iso-butanol, and space–time yield of the catalyst

To determine the influence of the reaction temperature and inlet concentrations of ethanol in the reaction mixture across several parameters of the process, such as ethanol conversion, iso-butanol yield, selectivity towards iso-butanol, and space–time yield of the 5 wt% Ni$_{99}$Pt$_1$/C catalyst, a series of experiments were carried out with the Ni$_{99}$Pt$_1$/C catalyst. In each case, the time on stream was constant and amounted to four hours. Fig. 3(a) shows that the ethanol conversion remained low with values of between 0% and a maximum of 2.50% in the temperature range between 120 °C and 150 °C. At temperatures over 150 °C, however, there was a significant increase in ethanol conversion to values of more than 10%. The maximum conversion of almost 13% was achieved at a reaction temperature of 180 °C and an initial ethanol concentration of 400 mmol l^{-1}. The diagram for the iso-butanol yield in part (b) of the figure shows similar trends, with the maximum yield also being approximately 13%. In the case of the selectivity towards iso-butanol (see part (c) of the

figure), significantly differing trends emerged. At reaction temperatures between 120 °C and 140 °C, the selectivity towards iso-butanol increased continuously to values of approx. 80%. In this temperature range, it depended only slightly on the inlet concentration of ethanol. The main by-products were acetaldehyde and 1-propanol. However, at reaction temperatures higher than 150 °C, excellent selectivities towards iso-butanol of 90–100% were achieved, if the inlet concentration of ethanol was between 100 mmol l^{-1} and 600 mmol l^{-1}. To achieve the most suitable selectivities, a reaction temperature of 165 °C should be selected. Then, a wide range for the inlet concentration of ethanol of between 100 mmol l^{-1} and 800 mm l^{-1} can be applied. Part (d) of the figure displays the space–time yield of the catalyst and shows that it rose significantly with increasing reaction temperatures. This stands in good agreement with previous findings, *e.g.*, with respect to ethanol conversion. However, diagram (d) also shows that the inlet concentration of ethanol had a stronger impact on the space–time yield than was found in the cases of ethanol conversion and iso-butanol yield. While highest ethanol conversions and iso-butanol yields, respectively, were achieved at ethanol concentrations in the range from 200 mmol l^{-1} to 550 mmol l^{-1} at corresponding reaction temperatures between 170 °C and 180 °C, the most promising space–time yield, with a value of 4.24 mmol h^{-1} g^{-1}, was obtained at an ethanol inlet concentration of 600 mmol l^{-1} at the same reaction temperatures. The exact numbers relating to ethanol conversion, iso-butanol yield, selectivity towards iso-butanol, and the STY of the catalyst in Fig. 3(a)–(d) can be found in the ESI† in Table S5.
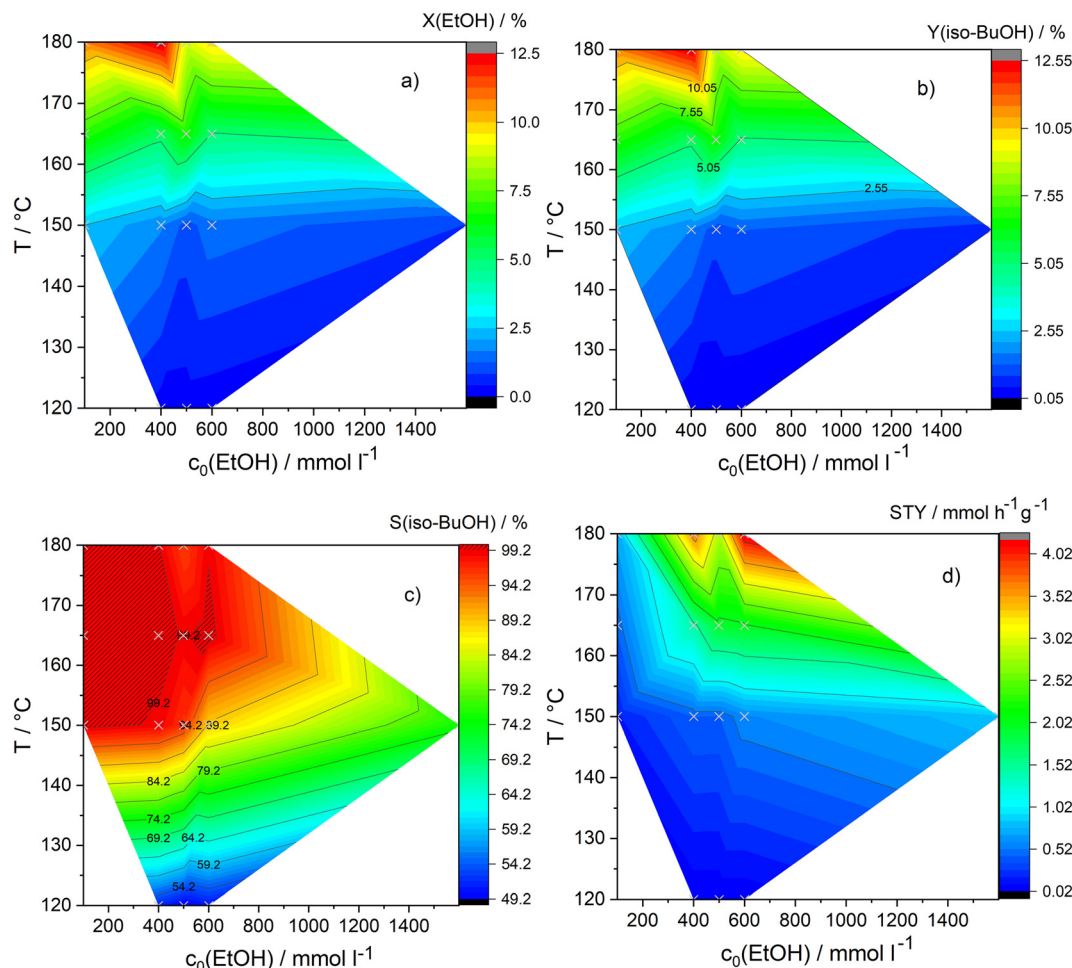
Kinetic measurements

To gain insight into the kinetics of the Guerbet reaction on the 5 wt% Ni$_{99}$Pt$_1$/C catalyst, the method of initial reaction rates v_0 was applied, which utilizes the dependence of the initial reaction rate on the initial concentration of the respective reaction partners. It primarily aims to determine the reaction constant and the reaction orders of the educts. To be able to apply this method, the complex reaction mechanism of the Guerbet reaction shown in Fig. 1 was simplified using the following equation:

$$2CH_3OH + CH_3CH_2OH \rightarrow CH_3CH(CH_3)CH_2OH + H_2O \quad (10)$$

The application of this method is particularly favorable for slow reactions and chemical processes in which the reaction products have no influence on the reaction rate.

It must be emphasized that during the experiments conducted for this study, the reaction educt methanol acted not only as a reactant but also as a solvent, as all experiments were conducted in a methanolic solution. Methanol was therefore present in large excess and its concentration can be regarded as constant throughout the course of the reaction. From the kinetic point of view, this means that the reaction

Fig. 3 Conversion of ethanol (a), iso-butanol yield (b), selectivity towards iso-butanol (c), and the STY of the catalyst (d) as a function of the reaction temperature and inlet concentration of ethanol; catalyst: 5 wt% $Ni_{99}Pt_1$/C, m(catalyst) = 250 mg, d(powder) < 75 μm, V(reactor) = 70 ml, c(NaOH) = 450 mmol l^{-1}, c(n-decane) = 15 mmol l^{-1}; time on stream: 4 h, methanolic solution, measuring points are shown as crosses.

order of methanol was set to zero. To rule out the reaction constant and reaction order of ethanol, Fig. 4 displays the natural logarithms of the initial reaction rates v_0 for the formation of iso-butanol as a function of the natural logarithm of the initial ethanol concentration at different reaction temperatures. All experimental data for this figure are summarized in Table S6 in the ESI.† The linear regression of the data points results in a straight line for each group of experiments at constant temperatures with the following general equation:

$$\ln(v_0) = \ln(k) + a \cdot \ln(c_0(\text{ethanol})) \tag{11}$$

where "k" represents the pseudo-reaction constant and "a" stands for the pseudo-reaction order with respect to ethanol. Following exponentiation, four equations were obtained for the initial formation rates v_0, yielding iso-butanol:

$$T = 120\ °C \qquad v_0 = 0.19\ h^{-1} \cdot c_0(\text{EtOH})^{-0.05} \tag{12}$$

$$T = 150\ °C \qquad v_0 = 0.05\ h^{-1} \cdot c_0(\text{EtOH})^{0.58} \tag{13}$$
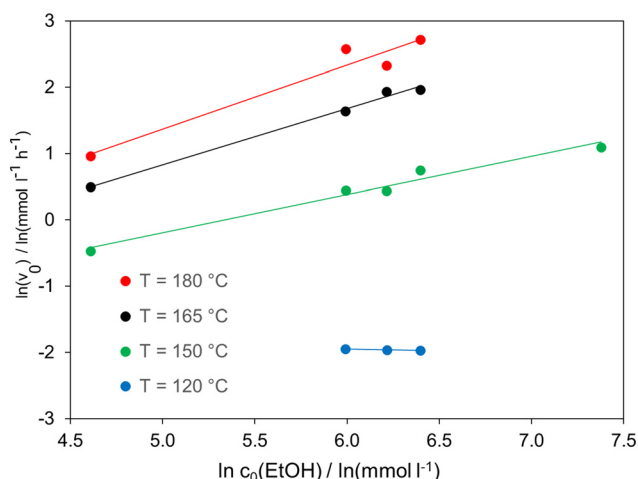
$$T = 165\ °C \qquad v_0 = 0.03\ h^{-1} \cdot c_0(\text{EtOH})^{0.85} \tag{14}$$

$$T = 180\ °C \qquad v_0 = 0.03\ h^{-1} \cdot c_0(\text{EtOH})^{1.00} \tag{15}$$

These equations were applied to calculate the time-dependent concentrations of iso-butanol at the different ethanol inlet concentrations according to the following equation (t stands for time on stream):

$$c(\text{iso-butanol}) = k \cdot t \cdot c_0(\text{ethanol})^a \tag{16}$$

In Fig. 5, the measured and calculated time-dependent concentrations of iso-butanol are exemplarily displayed at (a) a reaction temperature of 180 °C and an inlet ethanol concentration of 400 mmol l^{-1} and (b) at a reaction temperature of 150 °C and an inlet ethanol concentration of 500 mmol l^{-1}. A comparison between the values exhibits good agreement. The small deviations between measured and calculated concentrations of iso-butanol can be explained by the fact that the amount of catalyst used in the reaction varied slightly, whereas

Fig. 4 Natural logarithm of the initial reaction rates v_0 for the formation of iso-butanol as a function of the natural logarithm of the inlet concentration of ethanol at different reaction temperatures, catalyst: 5 wt% $Ni_{99}Pt_1$/C, m(catalyst) = 250 mg, d(powder) < 75 μm, V(reactor) = 70 ml, c(NaOH) = 450 mmol l^{-1}, c(n-decane) = 15 mmol l^{-1}, time on stream: 4 h, methanolic solution.

the reaction rate equations were standardized to 250 mg of catalyst. In addition, a slight conversion of ethanol to iso-butanol already took place during the reactor heating period, such that the starting condition without any formation of iso-butanol was not exactly met. All experimental data for this figure are summarized in Tables S7 and S8 in the ESI.†
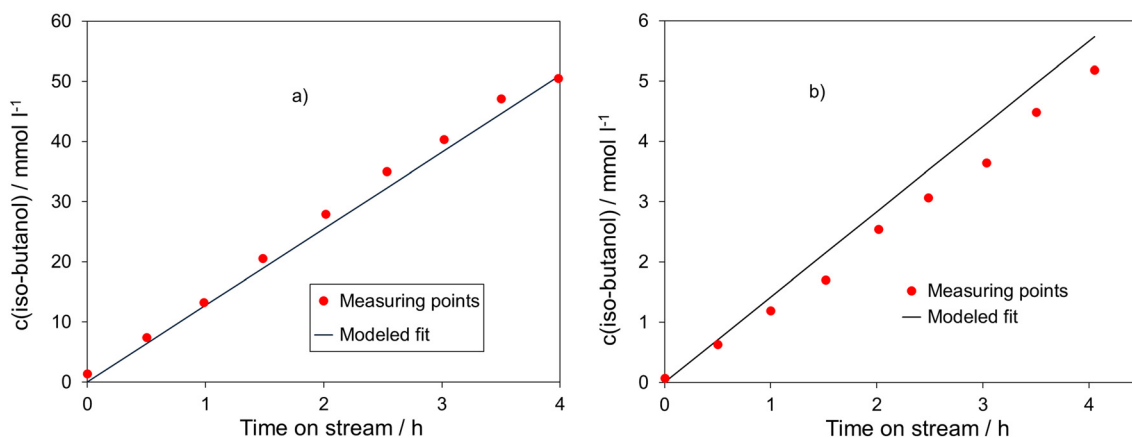
As can be derived from eqn (12)–(15), the pseudo-reaction orders "a" for the reaction temperatures significantly differ from each other. While there may still be an overlap between the values at 180 °C and 165 °C, respectively ($a = 1.00 \pm 0.17$ and $a = 0.85 \pm 0.05$, respectively), the pseudo-reaction order at 150 °C with $a = 0.58 \pm 0.06$ is significantly outside the scattering range. In Fig. 6, a linear increase in the reaction order can therefore be assumed in the temperature range from 120 °C to 180 °C. The measurement at 180 °C

represents an outlier. All experimental data for this figure are summarized in Table S9.†

Assuming that the determined pseudo-reaction orders are correct, it can be concluded that the mechanism for the formation of iso-butanol is dependent on the reaction temperature. This in term means that different reaction steps at different temperatures determine the rate. This observation has already been discussed in the literature. Different proposals have been made for the rate-determining steps.[11,40–42] Veibel and Nielsen[40] concluded that the dehydrogenation of benzyl alcohol was the rate-determining step at temperatures between 130 °C and 160 °C, whereas the aldol condensation between benzyl alcohol and potassium lactate determined the rate between 160 °C and 180 °C. Their catalysts used were copper bronze, RANEY® nickel, 10 wt% Pd/C, and Norit. In contrast, Kibby and Hall[11] identified the hydride transfer from the α-C atom of the alcohol to the neighboring PO_4^{3-} group of their hydroxyapatite catalyst as being the rate-determining step.
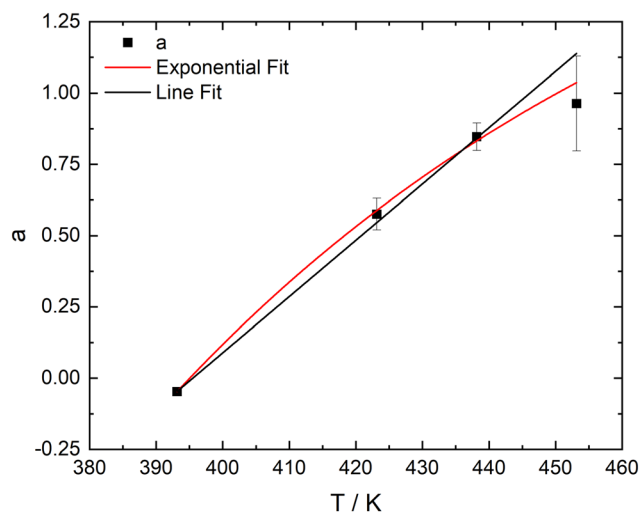
As already explained in the Experimental section above, the activation energy of the reaction can be determined for constant inlet concentrations of ethanol without determining the pseudo-reaction order "a," the pseudo-rate constant "k," and the pre-exponential factor "A" by means of eqn (8). The corresponding plot of the natural logarithm of the initial reaction rates v_0 against the reciprocal of the temperature then results in a straight line from the slope of which the activation energy can be calculated. These plots are exemplarily shown in Fig. 7 for ethanol inlet concentrations of 600 mmol l^{-1} and 400 mmol l^{-1}, respectively. All experimental data for these figures are summarized in Tables S10 and S11 in the ESI.† The calculated activation energies are listed in Table 2.

For concentrations between 400 mmol l^{-1} and 600 mmol l^{-1}, the activation energies were comparable in the range between approximately 110 kJ per mole and 120 kJ per mole. In the case of the lowest ethanol inlet concentration,

Fig. 5 Measured and calculated concentrations of iso-butanol as a function of time on stream: a) T = 180 °C and c_0(ethanol) = 400 mmol l^{-1}; b) T = 150 °C and c_0(ethanol) = 500 mmol l^{-1}, catalyst: 5 wt% $Ni_{99}Pt_1$/C, m(catalyst) = 250 mg, d(powder) < 75 μm, V(reactor) = 70 ml, c(NaOH) = 450 mmol l^{-1}, c(n-decane) = 15 mmol l^{-1}, methanolic solution.

This journal is © The Royal Society of Chemistry 2024

Catal. Sci. Technol., 2024, **14**, 7048–7060 | **7055**

Fig. 6 Pseudo-reaction order "*a*" for the formation of iso-butanol as a function of the reaction temperature, catalyst: 5 wt% $Ni_{99}Pt_1$/C, *m*(catalyst) = 250 mg, *d*(powder) < 75 μm, *V*(reactor) = 70 ml, *c*(NaOH) = 450 mmol l^{-1}, *c*(*n*-decane) = 15 mmol l^{-1}, time on stream: 4 h, methanolic solution.
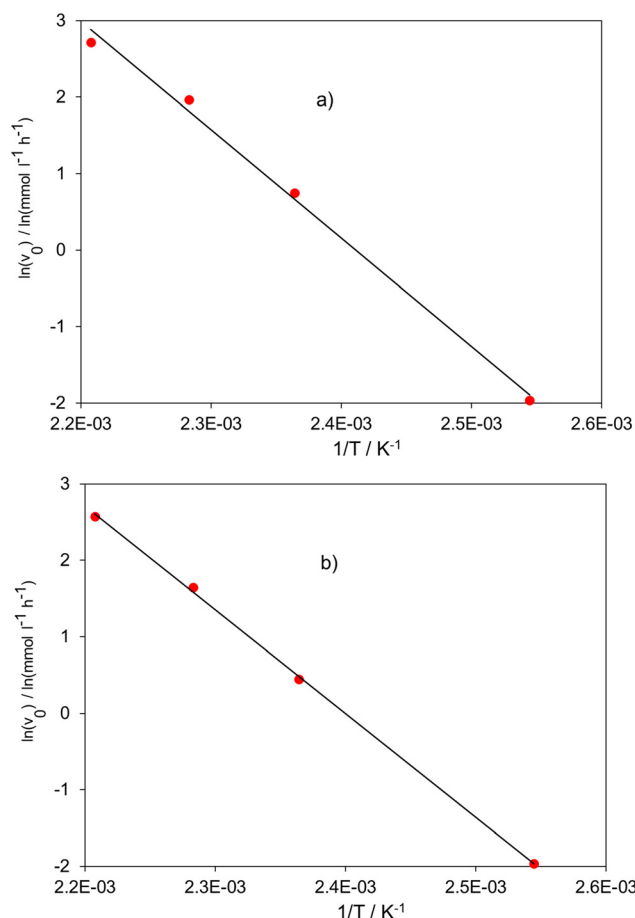
however, the value for the activation energy significantly decreased to approximately 76 kJ per mole.

Investigation of the metal surface after the reaction

To investigate the effect of the reaction conditions (reaction temperature, time on stream) on the appearance of the Ni and Pt catalyst particles being deposited on the activated carbon support, transmission electron microscopy (TEM) was utilized. In this respect, Fig. 8 shows TEM images of the fresh $Ni_{99}Pt_1$/C catalyst (see line a)) and of the samples used after test runs at 180 °C for four hours (see line b)) and at 150 °C for 24 hours of time on stream (see line c)). In each case, the first two columns display high-angle annular dark-field (HAADF)–TEM images at different magnifications, which are supplemented in the third column by energy-dispersive X-ray analysis (EDX) measurements. In all of these, the Ni particles are shown in green and the carbon carrier in orange. The fourth column displays high-resolution (HR)-HAADF–TEM images of the two used and fresh samples.

The HAADF images in row a) for the fresh $Ni_{99}Pt_1$/C catalyst show that the particles are statistically distributed and exhibit only slight signs of agglomeration. The particle size is approximately six nm and the particles are separated from each other. Pt could not be detected by EDX in either the fresh or the used catalysts. This fact is explained by a homogeneous distribution of Pt atoms in the catalyst material. The absence of Pt signals in the used catalysts indicates that there was no phase separation between Ni and Pt during the reaction.

Row b) shows, from left to right, an overview image, the magnification of the overview image, the corresponding EDX mapping, and an HR-HAADF–TEM of the $Ni_{99}Pt_1$/C catalyst, which was used in the iso-butanol synthesis at 180 °C for
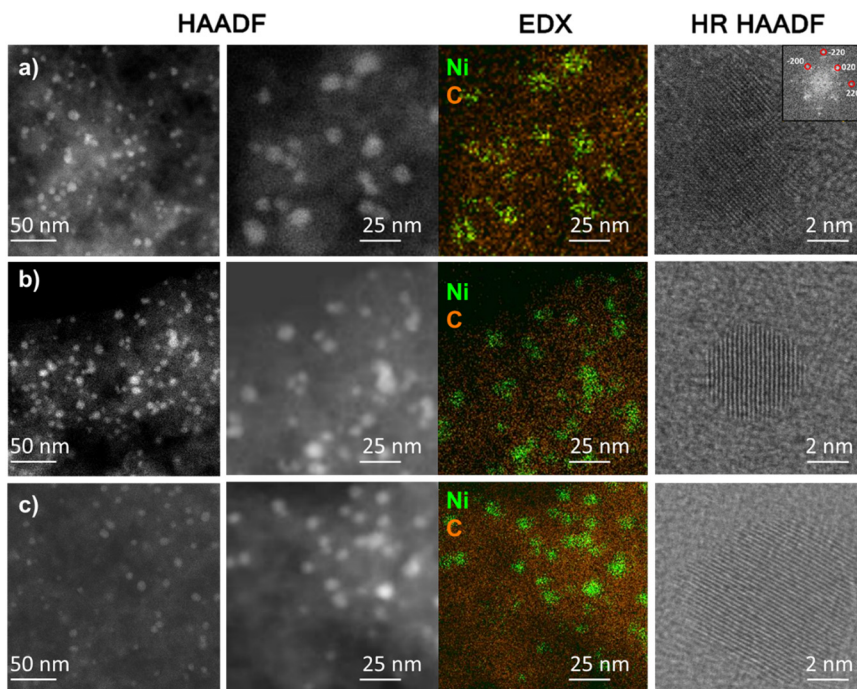

Fig. 7 Natural logarithm of the initial reaction rates v_0 for the formation of iso-butanol as a function of the reciprocal of the temperature at ethanol inlet concentrations of 600 mmol l^{-1} (a) and 400 mmol l^{-1} (b), catalyst: 5 wt% $Ni_{99}Pt_1$/C, *m*(catalyst) = 250 mg, *d*(powder) < 75 μm, *V*(reactor) = 70 ml, *c*(NaOH) = 450 mmol l^{-1}, *c*(*n*-decane) = 15 mmol l^{-1}, time on stream: 4 h, methanolic solution.

four hours of time on stream. The overview image shows that the particles are also statistically distributed. The magnification clearly indicates that the particles are similar in size to those of the fresh catalyst. The HR-HAADF image displays a crystalline particle with a lattice plane spacing of 0.2 nm. Row (c) presents the corresponding images of the catalyst, which was used in the *C*-methylation reaction at 150 °C for 24 hours on stream. All four figures clearly show that the outer appearance of the catalyst particles, as well as the EDX mapping, have not changed significantly compared to

Table 2 Activation energies for different inlet concentrations of ethanol, catalyst: 5 wt% $Ni_{99}Pt_1$/C, *m*(catalyst) = 250 mg, *d*(powder) < 75 μm, *V*(reactor) = 70 ml, *c*(NaOH) = 450 mmol l^{-1}, *c*(*n*-decane) = 15 mmol l^{-1}, time on stream: 4 h, methanolic solution

C_0^{EtOH} [mmol l^{-1}]	C [—]	E_a [kJ per mole]
600	34.16 ± 1.67	117.85 ± 5.89
500	31.95 ± 3.00	110.66 ± 10.60
400	32.44 ± 0.52	112.40 ± 1.84
100	21.25 ± 3.85	76.17 ± 14.03

7056 | *Catal. Sci. Technol.*, 2024, **14**, 7048–7060

This journal is © The Royal Society of Chemistry 2024

Fig. 8 HAADF–STEM and EDX investigations of: a) fresh $Ni_{99}Pt_1/C$ catalyst. b) $Ni_{99}Pt_1/C$ catalyst after 4 h of time on stream at 180 °C. c) $Ni_{99}Pt_1/C$ catalyst after 24 h of time on stream at 150 °C.
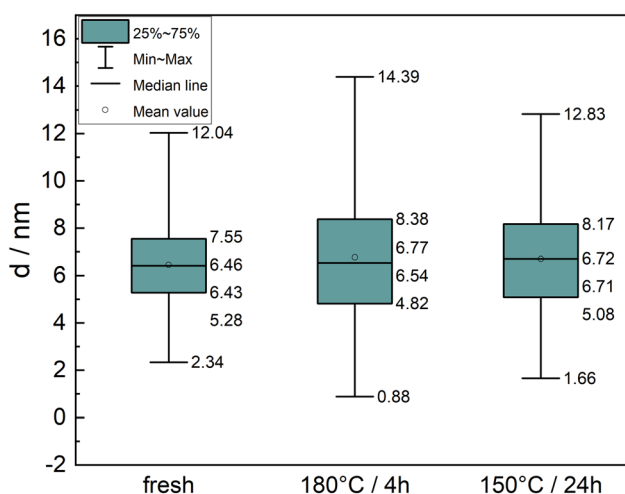
the catalyst samples from the first two lines. It can therefore be concluded from the analyses using TEM that there has been no ageing of the catalytically active species of the Ni_{99}-Pt_1/C catalyst during the iso-butanol synthesis.

Fig. 9 displays the particle size distributions of the different fresh and spent catalyst materials as a box plot. It shows that the particle size distribution of the fresh catalyst was in the range between 2.34 nm and 12.04 nm. The second and third quartiles ranged from 5.28 nm to 7.55 nm. The median particle size was 6.43 nm (N = 375). For the catalyst used in the reaction at 180 °C for four hours, the values of the particle sizes ranged from 0.88 nm to 14.39 nm. The second and third quartiles were further apart than for the fresh catalyst and ranged from 4.82 nm to 8.38 nm. Compared to the fresh catalyst, the median was only slightly higher, at 6.54 nm (N = 844). The dispersion of the particle sizes of the catalyst used in the reaction at 150 °C for 24 h ranged from 1.66 nm to 12.83 nm for the maximum particle size. However, the quartiles were now in a range from 5.08 nm to 8.17 nm, with a median of 6.71 nm (N = 677). No trend can be recognized in the almost symmetrical box plots that would suggest that the particle sizes increased with the reaction temperature or time on stream.

Classification of the $Ni_{99}Pt_1/C$ catalyst within the group of Guerbet catalysts

For this sub-section, literature data with respect to the formation rates for the Guerbet alcohols of the main representatives of the Guerbet catalysts was collected and used as benchmark. It is compared with the formation rates

for iso-butanol of the $Ni_{99}Pt_1/C$ from this work and several commercial monometallic activated carbon supported catalysts. The formation rates were calculated using eqn (9). These data are summarized in Table 3. For reasons of clarity, the table was arranged in descending order of reaction temperature.

Fig. 9 Box-and-whisker plot of the particle distribution from the TEM measurements of the $Ni_{99}Pt_1/C$ catalyst from Fig. 8. The top and bottom numbers give the whiskers and describe the range of the particle size distribution. The second numbers from the top and bottom indicate the particle size range, which comprises the second and third quartiles in the green box. The third number from the top indicates the mean value, which is also marked with a circle. The third number from the bottom indicates the median; sample sizes: N_{fresh} = 375, $N_{4h, 180°C}$ = 844, $N_{24h, 150°C}$ = 677.

This journal is © The Royal Society of Chemistry 2024

Catal. Sci. Technol., 2024, **14**, 7048–7060 | **7057**

Table 3 Formation rates for the Guerbet alcohols of the main representatives among the Guerbet catalysts compared with the formation rate for iso-butanol of the $Ni_{99}Pt_1/C$ and several commercial monometallic activated carbon supported catalysts

Number	Catalyst [—]	T [°C]	R [nmol m^{-2} s^{-1}]	Reference
1	Rb-LiX	420	4.3 μmol g^{-1} s^{-1}	12
2	β-Tri-calcium-phosphate	405	54.0	11
3	MgO	400	8.2	18
4	Mg–Al-oxide	400	3.6	31
5	CaO	397	1.1	26
6	K-CuMg$_5$CeO$_x$	300	0.8	14
7	Hydroxyapatite (Ca/P) = 1.67	300	13.0	11
8	Hydroxyapatite (Sr/P) = 1.70	298	6.5	19
9	Cu$_3$Ce/AC$_{batch}$	250	5.0	15
10	Cu$_3$Ce/AC$_{cont.}$	250	10.3	15
11	CuMg$_2$Al$_1$	230	93.4	13
12	Ir/NC	160	2.1	17
13	Ni$_{99}$Pt$_1$/C	165	0.78 ± 0.02	This work
14	Pd/C	150	0.028 ± 0.001	3
15	Rh/C	150	0.014 ± 0.001	3
16	Cu/C	150	0.153 ± 0.001	3
17	Ir/C	150	0.093 ± 0.002	3
18	Pt/C	150	0.94 ± 0.02	3

It becomes obvious from this table that most of the catalysts in entries 1 to 11 show higher values for the formation rate in comparison to the value of 0.78 nmol m^{-2} s^{-1} of the Ni$_{99}$Pt$_1$/C catalyst from this work (entry 13). However, they all worked at significantly higher reaction temperatures. The catalyst CuMg$_2$Al$_1$ with a high formation rate of 93.40 nmol m^{-2} s^{-1} being operated at 230 °C underwent deactivation within two to three hours of time on stream and a strong reduction in the number of acidic and basic centers compared to the fresh catalyst material.[13] In addition, it should be mentioned that Faba *et al.*[13] only used ethanol as educt whose reactivity as alkylation reagent is much higher than that of methanol as methylation reagent being used as co-educt for this work (molar ratio methanol to ethanol of 15 : 1 to favor the formation of iso-butanol).[3] In the case of the Cu$_3$Ce catalysts from entries 9 and 10, it was shown that the formation rate at a reaction temperature of 250 °C could be doubled as soon as the reaction was carried out as a continuous gas-phase reaction. This potential for increase has not yet been exploited for the NiPt catalyst from this work. In the work by Liu *et al.* in entry 12,[17] methanol and ethanol were converted to 1-butanol and iso-butanol in a liquid-phase reaction with water as the solvent. The Ir/NC catalyst showed good stability over a reaction period of 16 hours. However, it should be noted again that the molar ratio of ethanol to methanol was in the range of 6 : 1, which explains the higher formation rate of 2.1 nmol m^{-2} s^{-1}.

Compared to these data, the catalyst Ni$_{99}$Pt$_1$ catalyst prepared in this work showed a good formation rate for iso-butanol at a low reaction temperature of 165 °C and a low precious metal mass fraction in methanolic solution without deactivating over a period of 24 hours. It therefore shows potential for continuous operation. All commercial monometallic catalysts from entries 14–18 suffered from rapid deactivation (Pt/C) and/or much lower formation rates for iso-butanol.[3]

Conclusions

Bimetallic NiPt/C catalysts are active and stable materials for the synthesis of iso-butanol from ethanol/methanol blends *via* the Guerbet reaction scheme. When experimentally varying the reaction temperature, the inlet concentration of ethanol and time on stream, the reaction temperature was found to have the strongest impact on ethanol conversion, the selectivity towards iso-butanol, the yield of iso-butanol, and the space–time yield of the catalyst. Maximum ethanol conversion was achieved at 180 °C with 13% at an ethanol inlet concentration of 400 mmol l^{-1}. Above approximately 150 °C, selectivities towards iso-butanol in the range of 90–100% were achieved if the inlet concentration of ethanol was between 100 mmol l^{-1} and 600 mmol l^{-1}. To be able to set up a wide ethanol-to-methanol mixing ratio at the highest possible selectivities towards iso-butanol, a temperature range of 160–170 °C should be chosen. During the experimental evaluation of the reaction, no signs of deactivation of the catalyst were recognizable. This applies to all the temperature and concentration ranges investigated. The method of initial reaction rates was used to determine the kinetic parameters of the reaction. Due to the experimental condition that all experiments were carried out in a methanolic solution, the methanol concentration was considered constant. As a result, four rate laws were obtained. The corresponding reaction orders varied greatly and approached a value of one for higher reaction temperatures. For a temperature of 120 °C, a slightly negative reaction order was found, whereas for temperatures in the range of 150–180 °C, a directly proportional correlation with the ethanol concentration at the start of the reaction was determined. The concentrations of iso-butanol calculated from the rate laws showed good agreement with the experimental data. Without explicit calculation of the pseudo-reaction orders, the determined activation energy was

7058 | *Catal. Sci. Technol.*, 2024, **14**, 7048–7060

This journal is © The Royal Society of Chemistry 2024

in the range of approximately 110–120 kJ mol^{-1}. TEM and EDX measurements of the fresh and used catalysts showed that the fresh catalyst featured statistically-distributed particles without clear agglomeration. Most of these particles had a diameter of about six nm. The catalyst, after four hours of time on stream at 180 °C, also exhibited statistically-distributed particles of similar sizes. The HR-HAADF–STEM images showed crystalline particles with a lattice plane spacing of 0.2 nm. After 24 h, the catalyst on stream at 150 °C showed particles that did not differ from those described previously. No evidence of catalyst deactivation was found *via* the TEM and EDX measurements, which is in good agreement with the results from the experimental evaluation. It was also shown that the synthesis procedure can have a positive influence on the catalytic properties of the Ni$_{99}$Pt$_1$/C catalyst. By producing the catalyst *via* precipitation of Ni with NaOH as Ni(OH)$_3$ and subsequent impregnation with the Pt precursor, a catalyst was obtained that is characterized by a higher formation rate of iso-butanol and a higher selectivity towards iso-butanol.

Data availability

The data supporting this article have been included as part of the ESI.†

Author contributions

Conceptualization – Johannes Häusler and Joachim Pasel; funding acquisition – Ralf Peters; investigation – Johannes Häusler; methodology – Johannes Häusler and Joachim Pasel; supervision – Detlef Stolten; writing – original draft – Joachim Pasel; writing – review & editing – Joachim Pasel, Johannes Häusler, and Ralf Peters.

Conflicts of interest

There are no conflicts to declare.

Acknowledgements

References

1 S. Schemme, J. L. Breuer, R. C. Samsun, R. Peters and D. Stolten, Promising catalytic synthesis pathways towards higher alcohols as suitable transport fuels based on H$_2$ and CO$_2$, *J. CO$_2$ Util.*, 2018, **27**, 223–237.

2 J. Häusler, J. Pasel, C. Wöllhaf, R. Peters and D. Stolten, Dilute Alloy Catalysts for the Synthesis of Isobutanol via the Guerbet Route: A Comprehensive Study, *Catalysts*, 2024, **14**, 215.

3 J. Häusler, J. Pasel, F. Woltmann, A. Everwand, M. Meledina, H. Valencia, M. Lipińska-Chwałek, J. Mayer and R. Peters, Elucidating the Influence of the d-Band Center on the Synthesis of Isobutanol, *Catalysts*, 2021, **11**, 406.

4 J. Pasel, J. Häusler, D. Schmitt, H. Valencia, J. Mayer and R. Peters, Aldol condensation of acetaldehyde for butanol synthesis: A temporal analysis of products study, *Appl. Catal., A*, 2023, **324**, 122286.

5 J. Pasel, F. Woltmann, J. Häusler and R. Peters, Surface Redox Reaction for the Synthesis of NiPt Catalysts for the Upgrading of Renewable Ethanol/Methanol Mixtures, *Catalysts*, 2024, **14**, 77.

6 B. Iqbal, M. Saleem, S. N. Arshad, J. Rashid, N. Hussain and M. Zaheer, One-Pot Synthesis of Heterobimetallic Metal–Organic Frameworks (MOFs) for Multifunctional Catalysis, *Chem. – Eur. J.*, 2019, **25**, 10490–10498.

7 L. Nguyen, S. Zhang, L. Wang, Y. Li, H. Yoshida, A. Patlolla, S. Takeda, A. I. Frenkel and F. Tao, Reduction of Nitric Oxide with Hydrogen on Catalysts of Singly Dispersed Bimetallic Sites Pt1Com and Pd1Con, *ACS Catal.*, 2016, **6**, 840–850.

8 M. Ouyang, K. G. Papanikolaou, A. Boubnov, A. S. Hoffman, G. Giannakakis, S. R. Bare, M. Stamatakis, M. Flytzani-Stephanopoulos and E. C. H. Sykes, Directing reaction pathways via in situ control of active site geometries in PdAu single-atom alloy catalysts, *Nat. Commun.*, 2021, **12**, 1549.

9 H. Yu, W. Tang, K. Li, S. Zhao, H. Yin and S. Zhou, Enhanced Catalytic Performance for Hydrogenation of Substituted Nitroaromatics over Ir-Based Bimetallic Nanocatalysts, *ACS Appl. Mater. Interfaces*, 2019, **11**, 6958–6969.

10 W. Zhong, Y. Liu and D. Zhang, Theoretical Study of Methanol Oxidation on the PtAu(111) Bimetallic Surface: CO Pathway vs Non-CO Pathway, *J. Phys. Chem. C*, 2012, **116**, 2994–3000.

11 C. L. Kibby and W. K. Hall, Studies of acid catalyzed reactions: XII. Alcohol decomposition over hydroxyapatite catalysts, *J. Catal.*, 1973, **29**, 144–159.

12 C. Yang and Z. Y. Meng, Bimolecular condensation of ethanol to 1-Butanol catalyzed by alkali cation zeolites, *J. Catal.*, 1993, **142**, 37–44.

13 L. Faba, J. Cueto, M. Á. Portillo, Á. L. Villanueva Perales, S. Ordóñez and F. Vidal-Barrero, Effect of catalyst surface chemistry and metal promotion on the liquid-phase ethanol condensation to higher alcohols, *Appl. Catal., A*, 2022, **643**, 118783.

14 M. J. L. Gines and E. Iglesia, Bifunctional Condensation Reactions of Alcohols on Basic Oxides Modified by Copper and Potassium, *J. Catal.*, 1998, **176**, 155–172.

15 D. Jiang, X. Wu, J. Mao, J. Ni and X. Li, Continuous catalytic upgrading of ethanol to n-butanol over Cu–CeO2/AC catalysts, *Chem. Commun.*, 2016, **52**, 13749–13752.

16 M. León, E. Díaz and S. Ordóñez, Ethanol catalytic condensation over Mg-Al mixed oxides derived from hydrotalcites, *Catal. Today*, 2011, **164**, 436–442.

This journal is © The Royal Society of Chemistry 2024

Catal. Sci. Technol., 2024, **14**, 7048–7060 | **7059**

17 Q. Liu, G. Xu, X. Wang and X. Mu, Selective upgrading of ethanol with methanol in water for the production of improved biofuel—isobutanol, *Green Chem.*, 2016, **18**, 2811–2818.

18 A. S. Ndou, N. Plint and N. J. Coville, Dimerisation of ethanol to butanol over solid-base catalysts, *Appl. Catal., A*, 2003, **251**, 337–345.

19 S. Ogo, A. Onda, Y. Iwasa, K. Hara, A. Fukuoka and K. Yanagisawa, 1-Butanol synthesis from ethanol over strontium phosphate hydroxyapatite catalysts with various Sr/P ratios, *J. Catal.*, 2012, **296**, 24–30.

20 O. Fuchs and W. Querfurth, US2050788A, 1932.

21 W. Feng and L. Shushuang, CN108117480A, 2016.

22 T. Vanderspurt and J.-L. Kao, US5493064, 1994.

23 T. Vanderspurt, J. K. Russel and K. R. Miller, US5811602A, 1995.

24 C. Carlini, C. Flego, M. Marchionna, M. Noviello, A. M. Raspolli Galletti, G. Sbrana, F. Basile and A. Vaccari, Guerbet condensation of methanol with n-propanol to isobutyl alcohol over heterogeneous copper chromite/Mg–Al mixed oxides catalysts, *J. Mol. Catal. A: Chem.*, 2004, **220**, 215–220.

25 C. Carlini, M. Marchionna, M. Noviello, A. M. Raspolli Galletti, G. Sbrana, F. Basile and A. Vaccari, Guerbet condensation of methanol with n-propanol to isobutyl alcohol over heterogeneous bifunctional catalysts based on Mg–Al mixed oxides partially substituted by different metal components, *J. Mol. Catal. A: Chem.*, 2005, **232**, 13–20.

26 C. Carlini, M. Di Girolamo, A. Macinai, M. Marchionna, M. Noviello, A. M. Raspolli Galletti and G. Sbrana, Selective synthesis of isobutanol by means of the Guerbet reaction: Part 2. Reaction of methanol/ethanol and methanol/ethanol/n-propanol mixtures over copper based/MeONa catalytic systems, *J. Mol. Catal. A: Chem.*, 2003, **200**, 137–146.

27 T. Tsuchida, S. Sakuma and T. Yoshioka, US2009/0205246A1, 2009.

28 K. Kourtakis, M. B. d'Amore and L. E. Manzer, US7700813B, 2008.

29 Q. Liu, G. Xu, Z. Wang, X. Liu, X. Wang, L. Dong, X. Mu and H. Liu, Iridium Clusters Encapsulated in Carbon Nanospheres as Nanocatalysts for Methylation of (Bio) Alcohols, *ChemSusChem*, 2017, **10**, 4748–4755.

30 S. M. A. H. Siddiki, A. S. Touchy, M. A. R. Jamil, T. Toyao and K.-I. Shimizu, C-Methylation of Alcohols, Ketones, and Indoles with Methanol Using Heterogeneous Platinum Catalysts, *ACS Catal.*, 2018, **8**, 3091–3103.

31 T. Bligaard, J. K. Nørskov, S. Dahl, J. Matthiesen, C. H. Christensen and J. Sehested, The Brønsted–Evans–Polanyi relation and the volcano curve in heterogeneous catalysis, *J. Catal.*, 2004, **224**, 206–217.

32 P. Gupta, H. J. Drexler, R. Wingad, D. Wass, E. Baráth, T. Beweries and C. Hering-Junghans, P,N-type phosphaalkene-based Ir(i) complexes: synthesis, coordination chemistry, and catalytic applications, *Inorg. Chem. Front.*, 2023, **10**, 2285–2293.

33 W. Ueda, T. Kuwabara, T. Ohshida and Y. Morikawa, A low-pressure guerbet reaction over magnesium oxide catalyst, *J. Chem. Soc., Chem. Commun.*, 1990, 1558–1559.

34 R. L. Wingad, E. J. E. Bergström, M. Everett, K. J. Pellow and D. F. Wass, Catalytic conversion of methanol/ethanol to isobutanol – a highly selective route to an advanced biofuel, *Chem. Commun.*, 2016, **52**, 5202–5204.

35 E. S. Olson, R. K. Sharma and T. R. Aulich, Higher-alcohols biorefinery: improvement of catalyst for ethanol conversion, *Appl. Biochem. Biotechnol.*, 2004, **113–116**, 913–932.

36 A. Messori, A. Gagliardi, C. Cesari, F. Calcagno, T. Tabanelli, F. Cavani and R. Mazzoni, Advances in the homogeneous catalyzed alcohols homologation: The mild side of the Guerbet reaction, A mini-review, *Catal. Today*, 2023, **423**, 114003.

37 J. Pasel, J. Häusler, D. Schmitt, H. Valencia, M. Meledina, J. Mayer and R. Peters, Ethanol Dehydrogenation: A Reaction Path Study by Means of Temporal Analysis of Products, *Catalysts*, 2020, **10**, 1151.

38 S. Brunauer, P. H. Emmett and E. Teller, Adsorption of Gases in Multimolecular Layers, *J. Am. Chem. Soc.*, 1938, **60**, 309–319.

39 C. López-Olmos, M. V. Morales, A. Guerrero-Ruiz, C. Ramirez-Barria, E. Asedegbega-Nieto and I. Rodríguez-Ramos, Continuous Gas-Phase Condensation of Bioethanol to 1-Butanol over Bifunctional Pd/Mg and Pd/Mg-Carbon Catalysts, *ChemSusChem*, 2018, **11**, 3502–3511.

40 S. Veibel and J. I. Nielsen, On the mechanism of the Guerbet reaction, *Tetrahedron*, 1967, **23**, 1723–1733.

41 J. I. Di Cosimo, V. K. Díez, M. Xu, E. Iglesia and C. R. Apesteguía, Structure and surface and catalytic properties of Mg-Al basic oxides, *J. Catal.*, 1998, **178**, 499–510.

42 F. C. Meunier, J. Scalbert and F. Thibault-Starzyk, On the irrelevance of acetaldehyde self-aldolization during ethanol condensation at high temperatures over basic heterogeneous catalysts, *8th International Conference on Environmental Catalysis*, United States of America, Asheville, NC, 2014, pp. 24–27.